EUROPEAN ORGANIZATION FOR NUCLEAR RESEARCH

40,90

CERN/SI/Int.DL/69-13
30.12.69

NUMERICAL ANALYSIS OF THE PSB MULTITURN INJECTION

C. Bovet and D. Lamotte

CONTENTS

1. INTRODUCTION

L. Nielsen[1] began the study of the multiturn process for the PSB, using a "geometrical" step-by-step method. A numerical analysis, using the computer for tracing the trajectories of a great number of individual protons, is employed here for a more detailed study.

Compared to Nielsen's work, the present analysis has the following additional features:

- On the input side:
  - thin slices in longitudinal space (~ 0.1 of a revolution);
  - variable Q_H;
  - variable closed orbit displacement (non-linear in time);
  - smooth distribution of the Linac phase plane density;
  - introduction of the energy spread distribution;
  - variable septum thickness.
- On the output side:
  - time variation display of the capture efficiency;
  - optimization of the efficiency for a given pulse length;
  - study of the centre of gravity of charges along the circumference and during the whole process;
  - final density distribution in phase plane $\rho(x,x') = dn/d\epsilon\ (x,x')$;
  - final density distribution in phase plane $G(\epsilon) = dn/d\epsilon\ (\epsilon)$.

2. METHOD OF COMPUTATION

2.1 Linac beam

As shown by Lapostolle et al.[2] the Linac current versus emittance function is very well represented by the exponential function

$$I(\epsilon) = I_o\ (1 - e^{-\epsilon/\epsilon_o}) \qquad (1)$$

where I_o = current for full emittance

ϵ_o = emittance containing 63.2% of I_o.

The density distribution in phase plane is

$$P(\epsilon)\, d\epsilon = \frac{I_0}{\epsilon_0}\, e^{-\epsilon/\epsilon_0}\, d\epsilon \quad . \tag{2}$$

Furthermore the Linac phase plane density will be referred to as

$$J(\epsilon) = \frac{100\ n_s}{\epsilon_0}\, e^{-\epsilon/\epsilon_0} \tag{2'}$$

The norm of this function corresponds to the number of protons which would be injected in a 100% efficiency monoturn injection, as will become clear later on.

The maximum intensity I_0 is irrelevant in our computation since we are interested in relative values of intensities only (for efficiency or brilliance). Generally, $\underline{\epsilon_0}$ *) will be put equal to 10 mrad mm. There is also an energy spread supposed to be a Gaussian distribution with a r.m.s. value $\underline{\Delta p/p}$.

At the downstream end of the inflector septum the Linac beam is centred at a distance $\underline{di}$ to the septum, with an angle $\underline{dip}$, and it is focused with an ellipse axis ratio $\underline{\beta i}$.

For the numerical treatment, with given values of the parameters ϵ_0, $\Delta p/p$, di, dip, βi, about 10,000 protons are taken with random initial conditions. The random parameters are the phase plane coordinates of each proton at the injection point

$$\begin{pmatrix} x \\ x' \\ \Delta p/p \end{pmatrix}$$

which are given by

$$\beta i\ x'^2 + \frac{1}{\beta i}\, x^2 = \epsilon \ , \tag{3}$$

$$\frac{\beta i\ x'}{x} = \tan \psi \ . \tag{4}$$

ϵ is taken with a probability distribution given by Eq. (2),
ψ has a uniform probability between 0 and 2π.

---

*) Underlined quantities are input variables of the computer program.

2.2 PSB model

The ellipse acceptance has a surface πA, an axis ratio β and is supposed upright*) at injection point. Further numerical computations are performed in a phase plane with x' scaled up by β so that betatron oscillations are circular with a phase advance $2\pi Q$ per revolution and a maximum amplitude $r_A = \sqrt{\beta A}$ (see Fig. 1).

The closed orbit of a proton at time t is $d(t) + \alpha_p \, p/p$, where $d(t)$ is the parallel closed orbit displacement during injection.

2.3 Multiturn process

The various time parameters are as follows:

t_f = total duration of injection process (particles are only available from the Linac during an interval $t_m \leq t_f$);

t_m = duration of the Linac pulse per ring;

t_{rev} = revolution time, thus there will be $n_t = t_m/t_{rev}$ turns actually injected.

The injected particles belong to n_s slices ($n_s \leq 100/n_t$) which are added azimuthally to fill one revolution (see Fig. 2). The time t is quantized in steps $dt = t_{rev}/n_s$. 100 protons are injected at time $t = 0$ into slice 1, at $t = dt$ into slice 2, etc.; at $t = t_{rev}$, 100 new protons are additionaly put into slice 1 again, and so on.

Any proton may be lost at any revolution when passing the injection point either by hitting the septum or by leaving the PSB acceptance.

The closed orbit parallel displacement is a function of time

$$d(t) = do - (do - df) \frac{1 - e^{-\gamma t}}{1 - e^{-\gamma t_f}} \qquad (5)$$

where do is the initial closed orbit displacement.

$df = dse - ds - r_A$ is the final value of c.o. displacement,

γ is a shape parameter (see Fig. 3).

---

*) This is strictly true for the middle of the injection straight section. The betatron phase shift to the injection point is about 10°.

2.4 Summary of input parameters

Table 1

System	Parameter	Range of values	Units
Linac beam	ϵ_o	5.0 , 8.0 , 10.0	mrad mm
	βi	0.6 - 4.0	m
	di	2.0 - 8.5	mm
	dip	- 2.0 - 2.0	mrad
	$\Delta p/p$	0 - 4.0	‰
PSB	A	130.0	mrad mm
	Q_H	4.1 - 4.9	
	β_H	5.8 - 4.5	m
	α_p	1.52 - 1.04	m
Multiturn process	t_f	10.0 - 60.0	μsec
	t_m	7.0 , 20.0 , 34.0	μsec
	($\sim n_t$)	4.0 , 12.0 , 20.0	
	dse	40.0	mm
	ds	0 - 2.0	mm
	do	40.0 - 60.0	mm
	γ	0 - 0.2	

2.5 Output facilities

a) Listed quantities

d(t) (for each value of t),

H(t) = number of protons injected at time t, accepted and preserved until the end of the process,

SOM = $\int_{t_o}^{t_o+t_m} H(t)\,dt$, $(0 \leq t_o)$; and t_o is chosen in order to get a maximum for SOM, i.e. for EFF (see Fig. 6)

$G(\epsilon) = \frac{dn}{d\epsilon}(\epsilon)$ is the phase plane density distribution of all protons surviving at the end of the process,

DOEFF = $d(t_o)$,

EFF = $\frac{SOM}{100} \cdot \frac{dt}{t_m}$, i.e. optimum efficiency during t_m.

b) Graphical output

H(t) $(0 < t < t_f)$,

G(ϵ) $[\int_0^A G(\epsilon)\, d\epsilon = SOM]$ together with the monoturn phase plane density, $J(\epsilon)$ given by Eq. (2'),

$\rho(x,x')$: phase plane density in one slice,

$\Sigma\rho(x,x')$: phase plane density of all slices transferred back to the injection point.

c) Plotted output (CALCOMP)

c(t) : evolution in phase plane at the injection point of the centre of gravity of surviving protons in the present slice,

Σc(t): idem for all slices transferred back to the injection point.

3. MAXIMUM EFFICIENCY

3.1 Optimization

Each value of EFF in this optimization will be a result of tracing about 10,000 protons, evaluating a distribution H(t) (like that shown in Fig. 5) and optimizing EFF by choosing the most efficient interval of length t_m during t_f (see Fig. 4).

Three parameters will be considered as fixed:

$$A = 130 \text{ mrad mm} \; ; \qquad dse = 40 \text{ mm} \; ; \qquad \gamma = 0$$

(closed orbit displacement linear in time).

The injection parameters βi, di, dip are free for the optimization as well as do and t_f which affect the function d(t).

Let us optimize for the following set of values (see Table 2). do is not an important parameter for the optimization provided its value is chosen large enough, the optimum solution will be found for a certain value of t_f.

Figures 5 and 6 show the function EFF versus t_o, t_f, βi, di, dip. In principle each point of these graphs gives the efficiency EFF versus one parameter and optimized on the other three.

Table 2

t_m	7	20	34
n_t	~4	~12	~20
t_f	14	34	55
$\Delta p/p$	2	2	2
Q	4.7	4.7	4.7
ds	1	1	1
do	50	50	55

3.2 Variation of parameters

The most significant result is the efficiency versus Q. For $Q = n \pm 1/i$ ($i = 2, 3, 4$) the efficiency drops due to the fact that accepted protons come in phase again after i revolutions at the injection point and are more likely to be lost on the septum than protons out of phase. This effect is shown on Fig. 6 where the influence of $\Delta p/p$ and ds are also presented.

The build-up current versus t_m for different values of ϵ_o is shown in Fig. 7. These values reached with the other parameters given by Table 1 are to be compared with Nielsen's results (dashed curve) and the analytic formulation of Ref. 3 (black curves).

4. PHASE PLANE DENSITY

Figures 8 and 9 show phase plane density distributions where printed numbers (1-9) represent number of particles. The following parameters are fixed:

$$\epsilon_o = 10\,, \quad \beta i = 2\,, \quad di = 3.5\,,$$
$$dip = 0\,, \quad \Delta p/p = 0\,, \quad A = 130\,,$$
$$dse = 40\,, \quad ds = 2\,, \quad \gamma = 0.0001\,,$$
$$t_f = 30\,, \quad t_m = 20\,,$$

and the Q-values are respectively 4.6 and $4\frac{2}{3}$.

In Fig. 8 is shown the density of one slice, i.e. $\rho(x,x')$. Septum cuts are clearly visible, and such figures look like Nielsen's ones but for different Q-values. On the contrary, Fig. 9 shows the density $\Sigma\rho(x,x')$, where all particles are traced back to the phase plane at the injection point. The septum cuts disappear, but the non-uniform filling at $Q = 4\frac{2}{3}$ is striking.

4.1 Maximum brilliance

It might be interesting for the filling of the ISR as well as for other reasons to get a maximum intensity in a PSB acceptance smaller than the nominal acceptance A = 130.

The pulse length t_m has been considered as a free variable and optimized for two cases A = 30 and A = 60, the other parameters being conserved, i.e.

$$\epsilon_o = 10 \ , \quad \Delta p/p = 2 \ , \quad dse = 40 \ , \quad ds = 1 \ , \quad \gamma = 0 \ .$$

Optimized values of βi, di, dip are taken from results of Section 3.

Figure 10 gives the phase plane densities (smoothed) of the PSB beam with a maximum brilliance compared to the Linac density, for three values of A.

The reduction of the densities near the acceptance edges is due to the non-zero energy spread. The effect of the septum thickness is specially important for small acceptances [ds = 0, $\bar{G}(A = 30) = 78\%$].

The mean density $\bar{G}$ or brilliance is given for each case on Fig. 10. One has

Linac:	I_o/ϵ_o	= 100%
PSB :	$\bar{G}(A = 30)$	= 57%
	$\bar{G}(A = 60)$	= 53%
	$\bar{G}(A = 130)$	= 54%

These values are optimized on the pulse length t_m for a septum thickness of ds = 1 mm. Figure 11 shows the sensitivity of the brilliance to values of t_m.

4.2 Uniform density

The density distributions shown on Fig. 10 might not be the best ones to fit space charge requirements. This density clearly depends on the rate

of change of the closed orbit d(t). According to different values of γ [see Eq. (5) and Fig. 4] resulting density shapes are shown on Fig. 12. γ seems to be sufficiently effective to allow for a valuable optimization or study of the injection at high intensity.

4.3 Coherent oscillations

As suggested by M. Weiss[4], the multiturn process may fill the phase plane in such a way that the centre of gravity of charges does not coincide with the closed orbit along the circumference of the machine.

This might result in coherent oscillations which cannot be compensated for by an adjustment of the injection steering dipoles. Figure 13 shows a trajectory in phase plane each point of which is the centre of gravity of the slice presently at injection point. One notices a discontinuity after each revolution. The amplitude of the excursion in phase plane is a function of t_m as seen from Fig. 13, but in any case it seems to be rather negligible in the last revolution compared to the beam size.

What remains of this at the end of the multiturn process can be seen by the position and shape of centres in the last revolution (thick line on Fig. 13). This last revolution is entirely subsequent to the end of the process (marked by a black circle). Later on, the polygon marked by the black line will no longer change shape, but will be rotated around the closed orbit (centre of phase plane). The beam will therefore show a peculiar coherent oscillation with phase and amplitude varying periodically in time.

5. CONCLUSIONS

The numerical analysis presented here confirms previous estimates[1] and the analytical approach within the limits stated for zero septum thickness[3]. Significant results are as follows:

- The horizontal betatron matching is not critical and the same value $\beta i \sim 2m$ seems to be good for any number of turns (Fig. 5).
- The coordinates (di, dip) of the injection trajectory must be chosen more carefully (Fig. 5) (dip must be adjusted relative to the actual closed orbit).
- The optimum efficiency versus t_f is very sharp (Fig. 5). (t_f controls the rate of closed orbit displacement during the injection.)
- Values of Q also affect the efficiency as shown on Fig. 6.
- The energy spread has a small and almost linear influence on efficiency.

- On the other hand 1 mm septum thickness reduces by 10% the efficiency of a 34 μsec injection (Fig. 6).
- By suitable adjustment of parameters, brilliances up to 53% and 57% of the central brilliance I_0/ϵ_0 of the Linac beam can be obtained for an H-acceptance limited respectively to A = 60 and A = 30 (Fig. 13).
- In the optimization of brilliance, a large number of turns is not very useful owing to a saturation. For A = 30 there is even a maximum at t_m = 15 μsec.
- Different values of γ allow us to play with the phase plane density distribution $G(\epsilon)$ (Fig. 12).
- The coherent oscillations resulting from the process are scarcely observable (they depend upon t_m) (~ 0.2 mm).

* * *

REFERENCES

1) L. Nielsen, Investigation of the possibilities of multiturn injection into the booster, CERN Internal Report MPS/Int-LIN 67-8.

2) P.M. Lapostolle et al., Intensity-dependent effects and space charge limit investigation on CERN linear injector and synchrotron, CERN 68-35 (1968).

3) C. Bovet, Filling the PSB with the Linac beam, CERN Internal Note SI/Note - DL/69-15.

4) M. Weiss, Private communication.

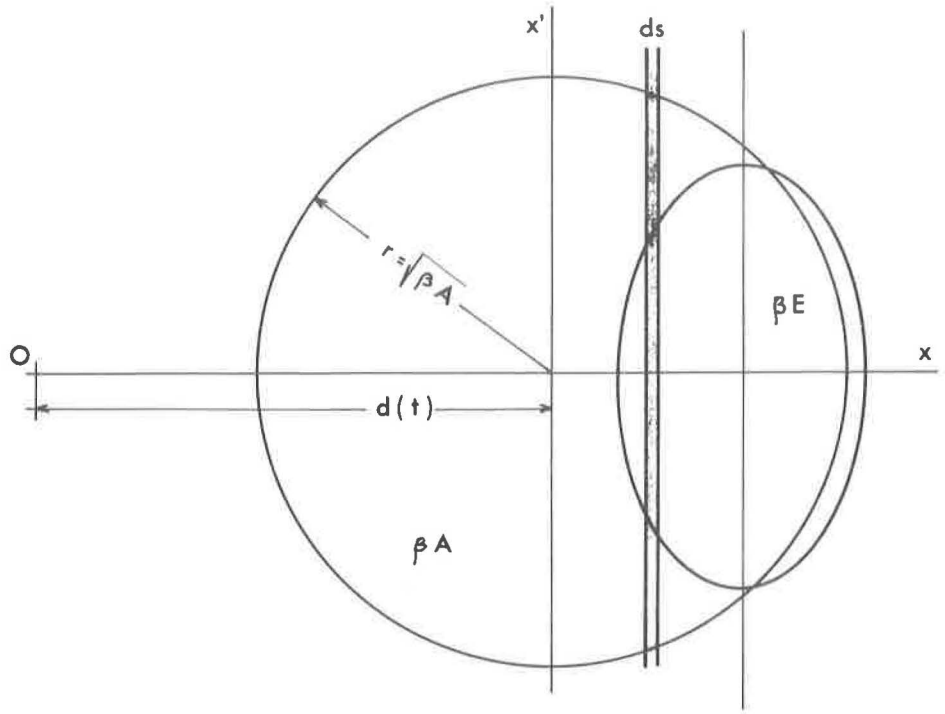
x'
ds
r=√βA
βE
O
x
d(t)
βA

Fig. 1

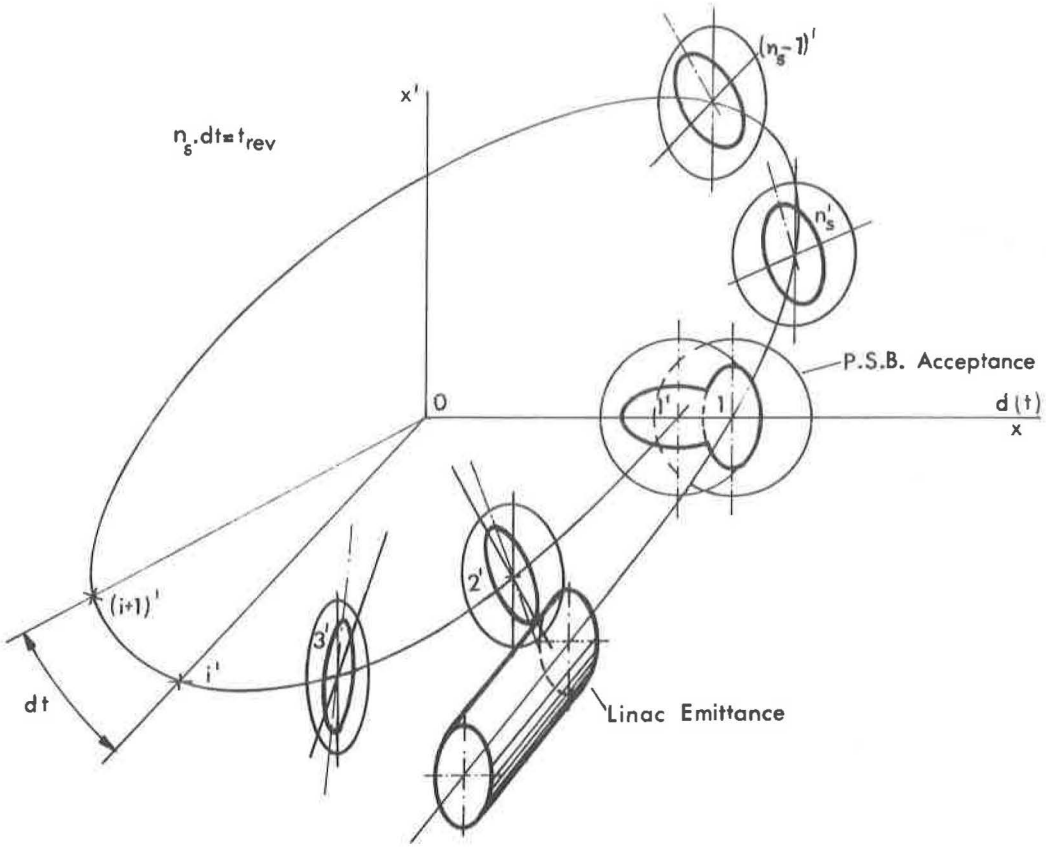
(n_s-1)'
x'
n_s.dt=t_rev
n'_s
P.S.B. Acceptance
0
1'
1
d(t)
x
(i+1)'
2'
3'
i'
dt
Linac Emittance

Fig. 2

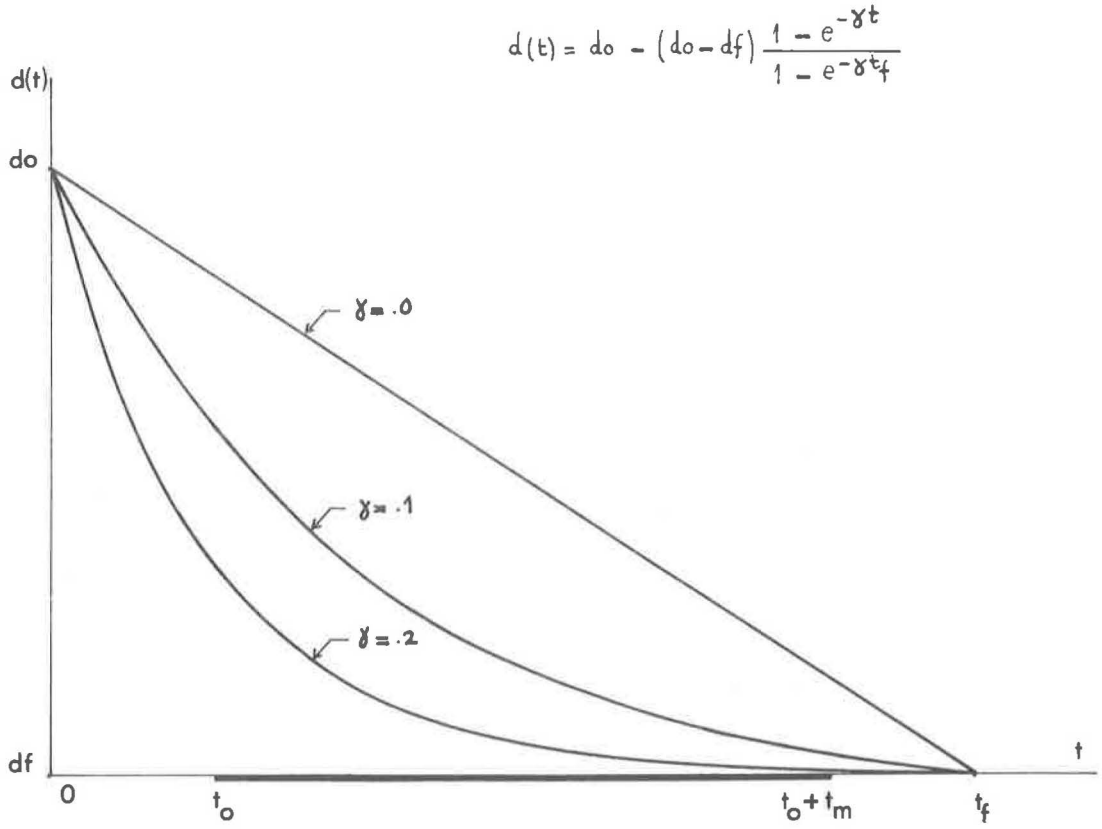
$d(t) = do - (do - df)\frac{1 - e^{-\gamma t}}{1 - e^{-\gamma t_f}}$
d(t)
do
df
0
t_o
$t_o + t_m$
t_f
t
$\gamma = .0$
$\gamma = .1$
$\gamma = .2$

Fig. 3

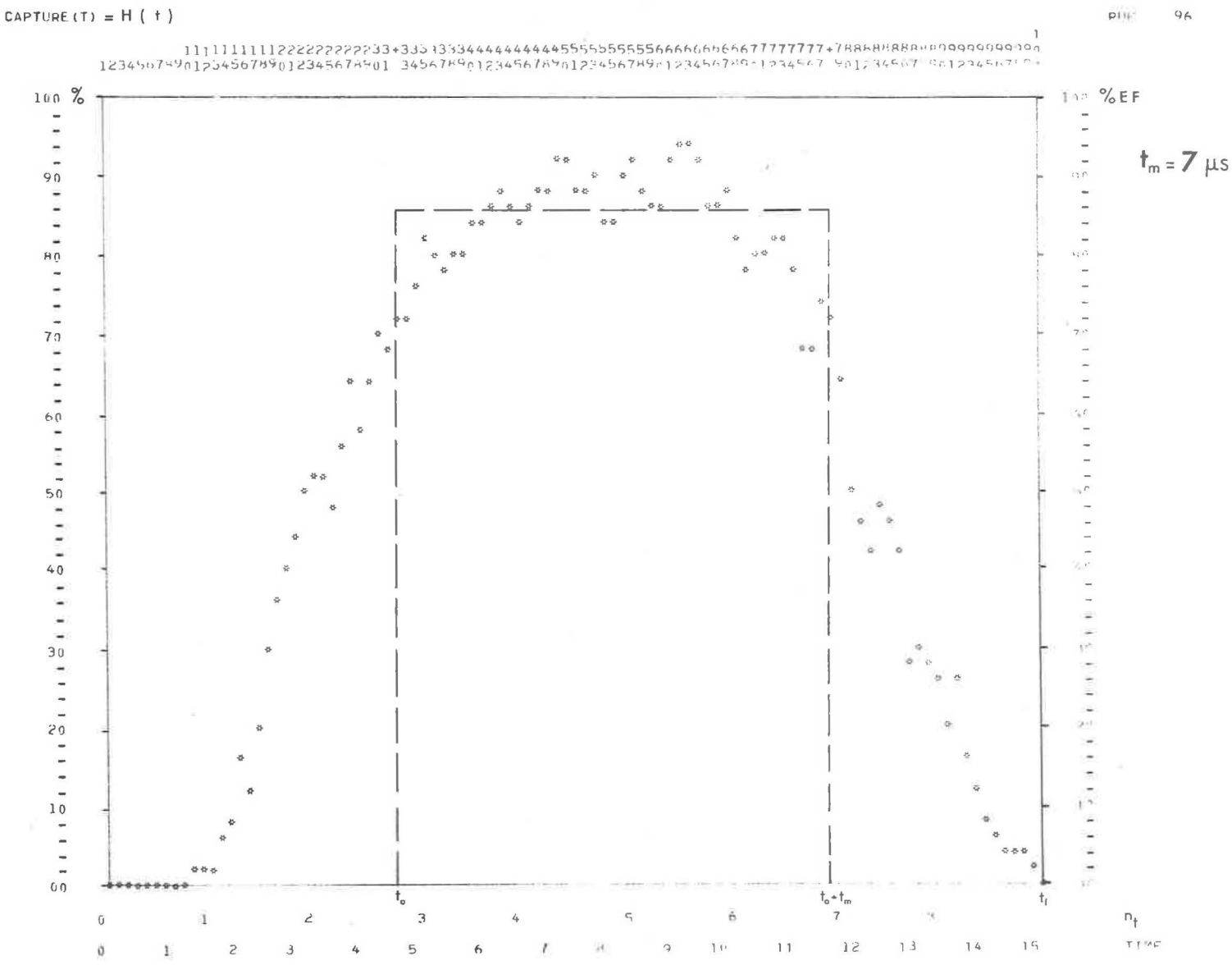
CAPTURE (T) = H (t)
100 %
90
80
70
60
50
40
30
20
10
00
%EF
$t_m = 7\ \mu s$
t_o
$t_o + t_m$
t_f
n_t
TIME

Fig. 4

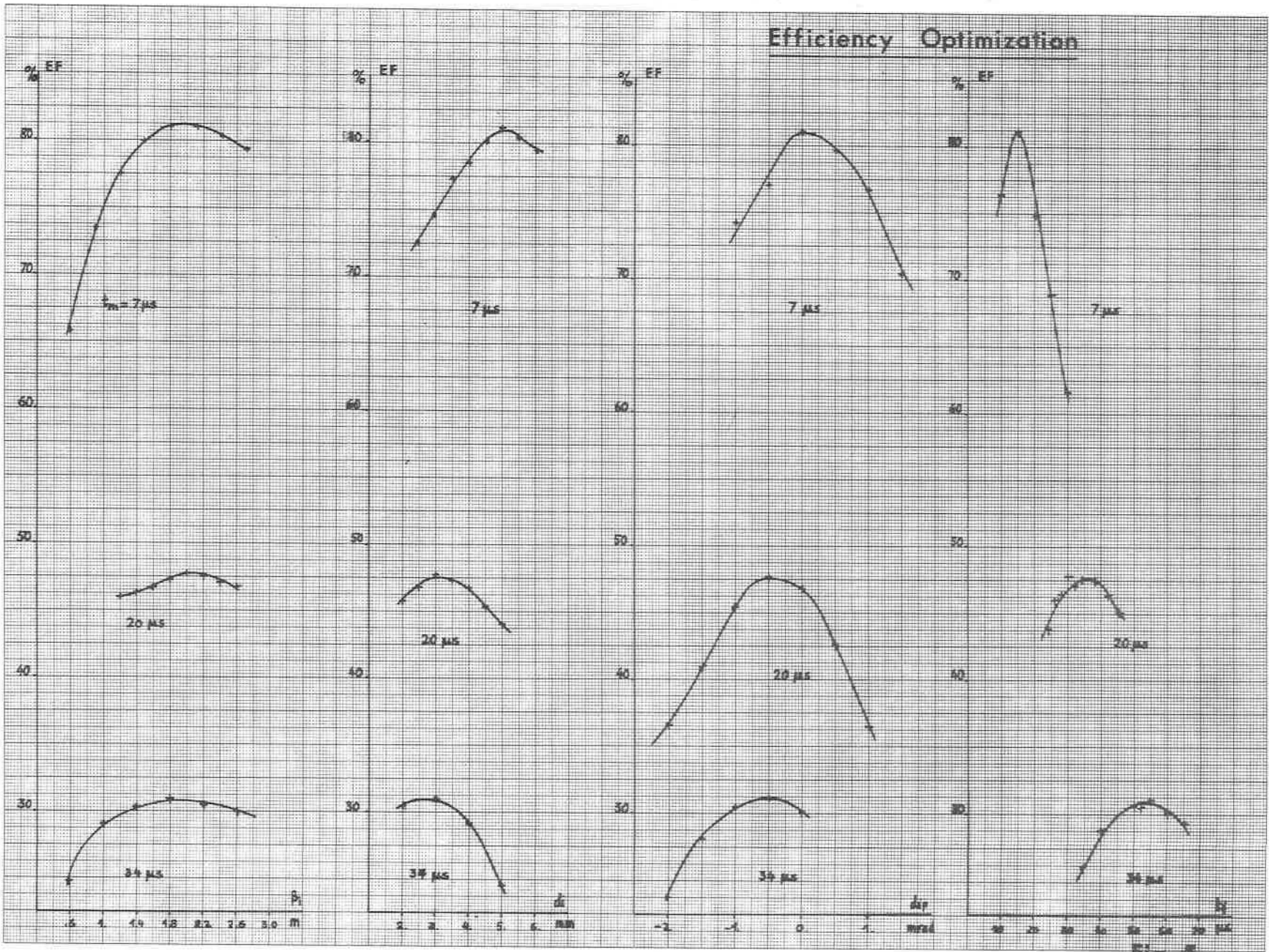
Efficiency Optimization
% EF
80
70
60
50
40
30
t_m = 7 µs
20 µs
34 µs
p_i
1.6 1.4 1.8 2.2 2.6 3.0 m
7 µs
20 µs
34 µs
d_i
2 3 4 5 6 mm
7 µs
20 µs
34 µs
d_{ep}
-2 -1 0 1 mrad
7 µs
20 µs
34 µs
t_{ep}
40 20 30 50 60 70 µs

Fig. 5

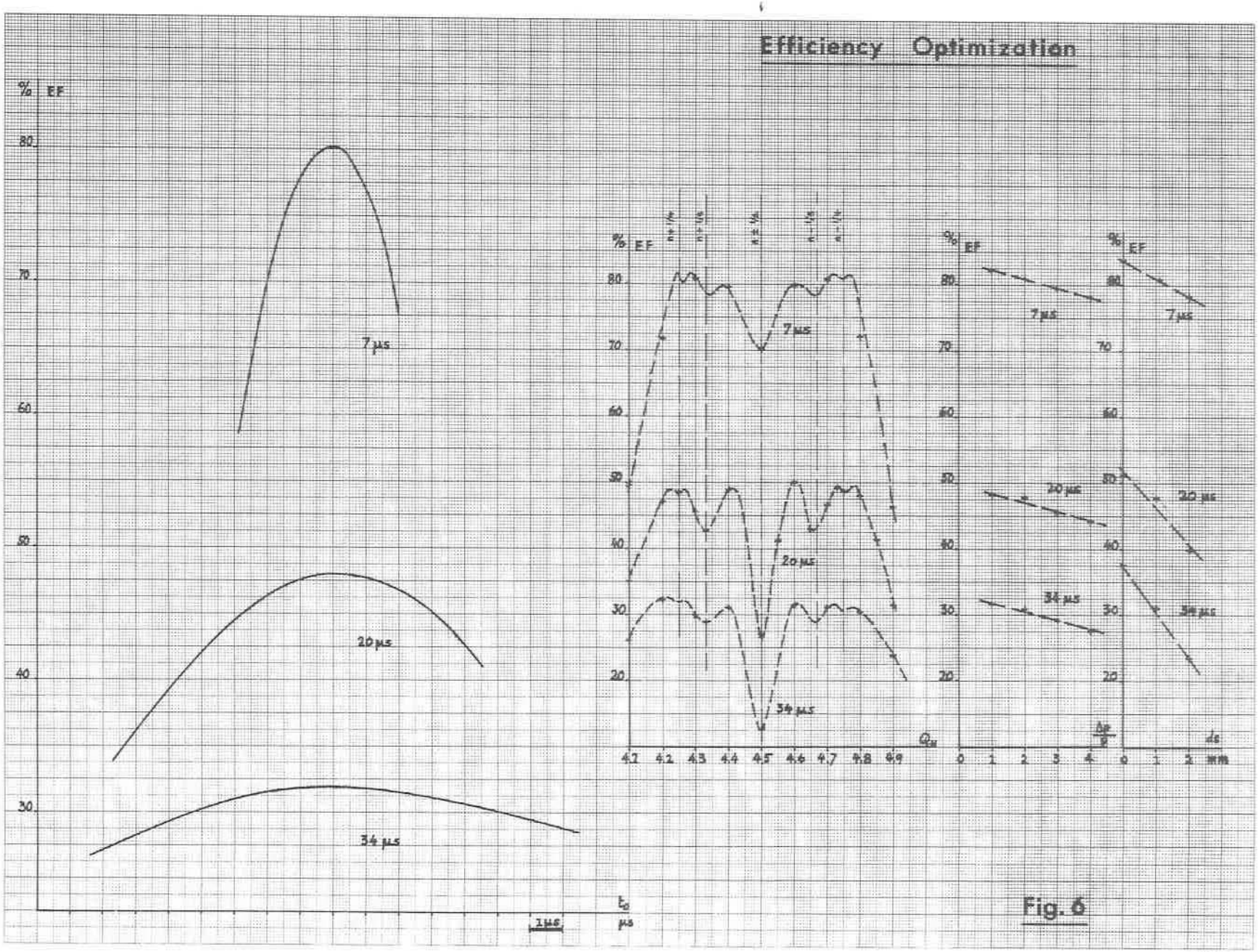
Efficiency Optimization
% EF
80
70
60
50
40
30
7 µs
20 µs
34 µs
1 µs
t_0
µs
Ω_M
4.1 4.2 4.3 4.4 4.5 4.6 4.7 4.8 4.9
$\frac{\Delta P}{P}$
Δs
0 1 2 3 4 0 1 2 3 mm

Fig. 6

CURRENT BUILD - UP

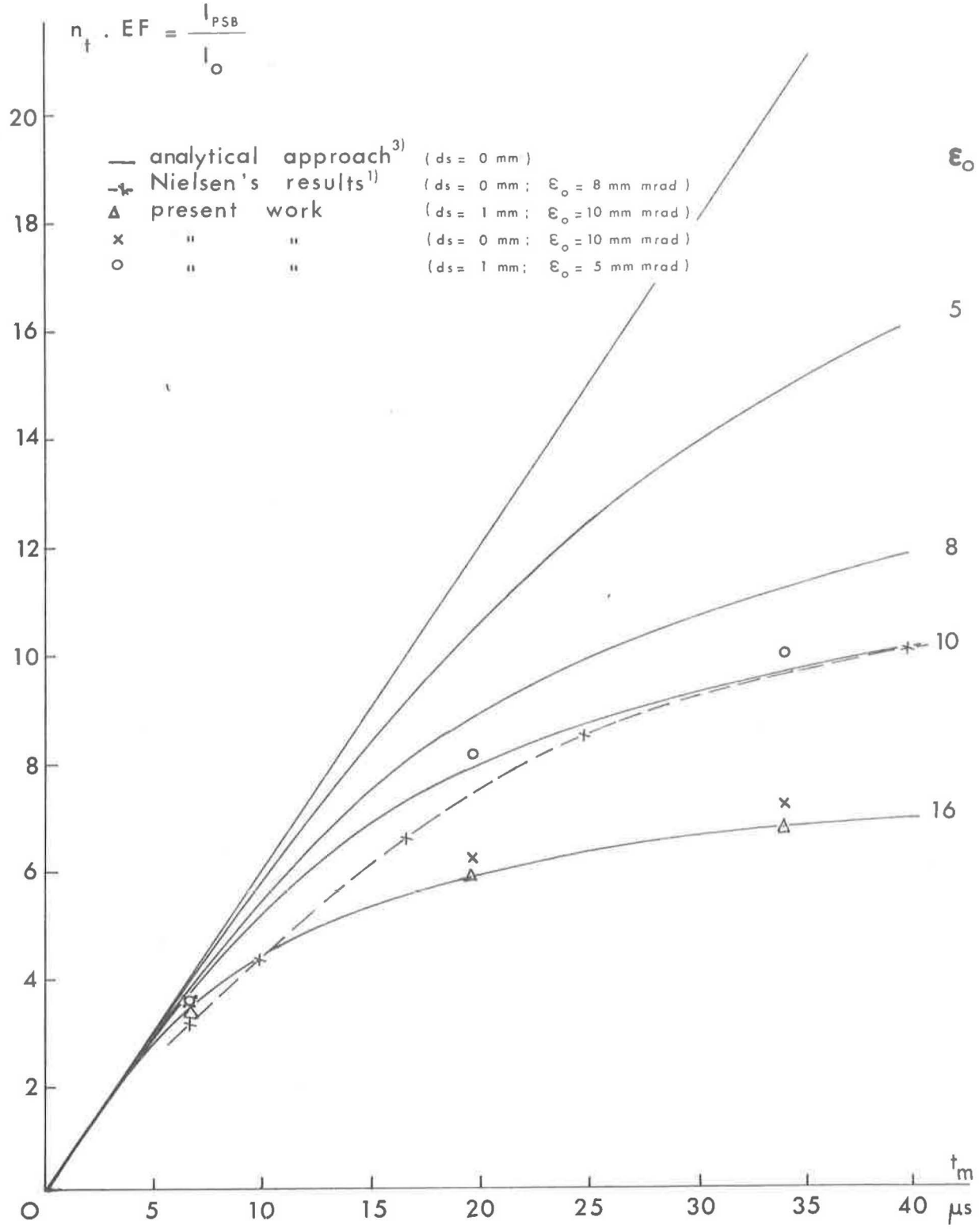

Fig. 7

ACCEPTANCE $Q = 4.6$ $t_m = 20$

$ds = 2$; $\frac{dp}{p} = 0.$

ACCEPTANCE $Q = 4\frac{2}{3}$ $t_m = 20$

$ds = 2$; $\frac{dp}{p} = 0.$

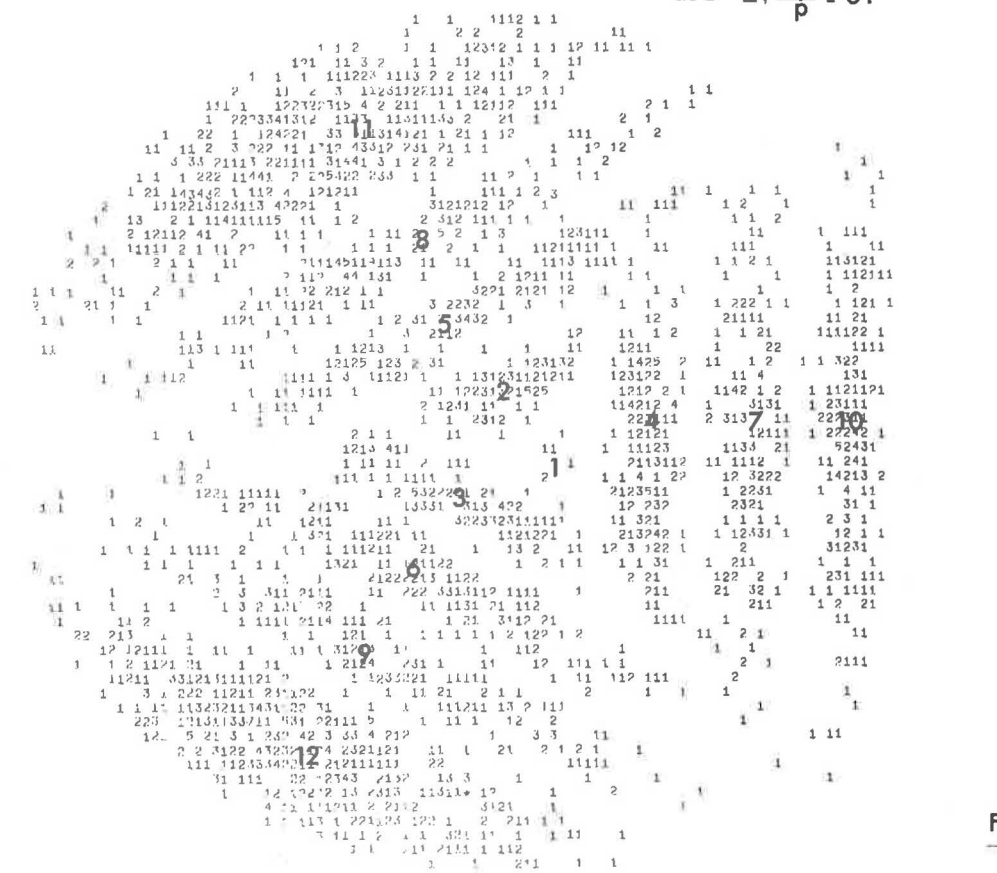

Fig. 8

ACCEPTANCE TOTALE $Q = 4.6$ $t_m = 20$

$ds = 2$; $\frac{dp}{p} = 0.$

ACCEPTANCE TOTALE $Q = 4\frac{2}{3}$ $t_m = 20$

$ds = 2$; $\frac{dp}{p} = 0.$

Fig. 9

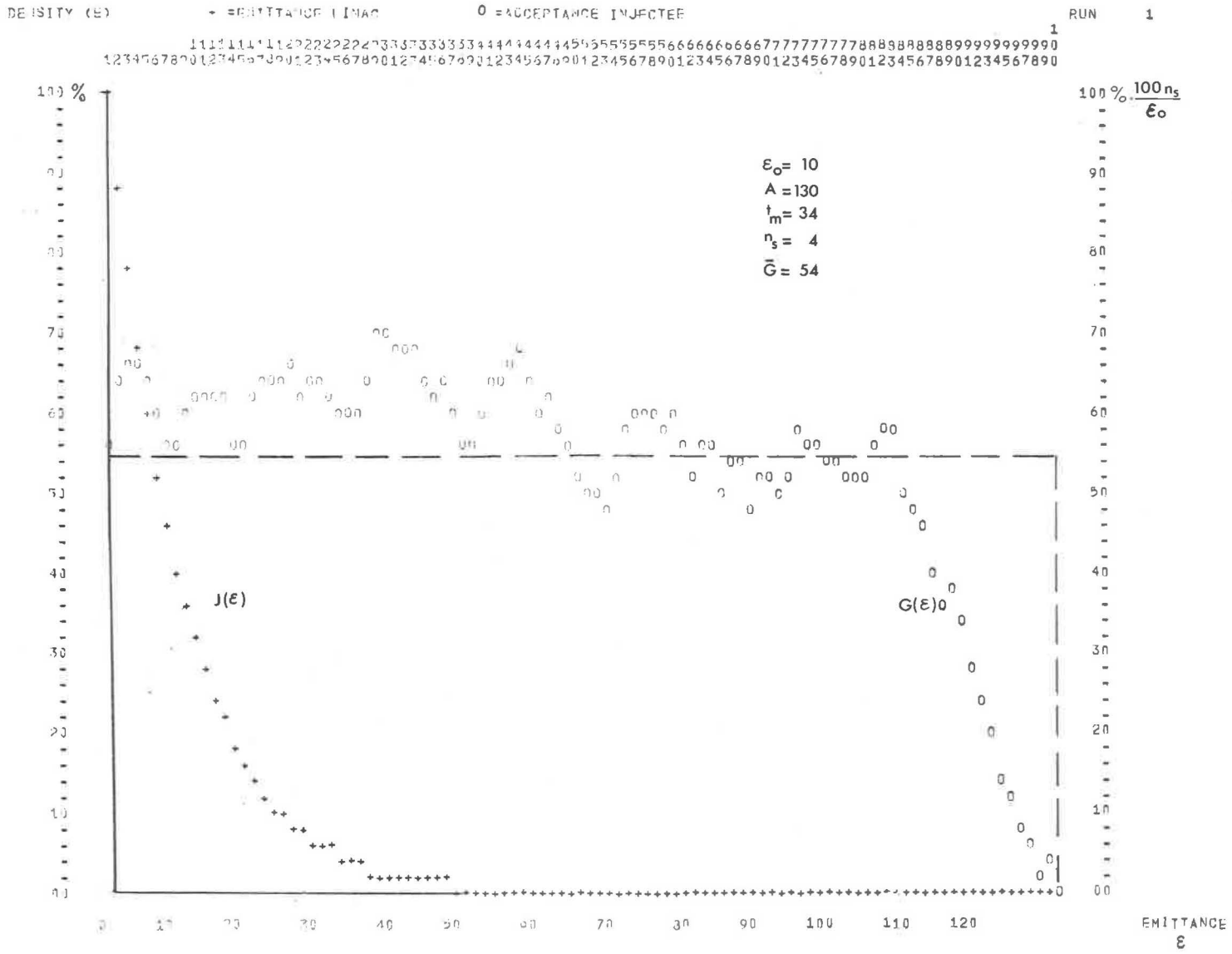
DENSITY (E)
+ =EMITTANCE LINAC
0 =ACCEPTANCE INJECTEE
RUN 1
100 %
$\frac{100\,n_s}{\varepsilon_o}$
ε_o= 10
A =130
t_m= 34
n_s = 4
$\bar{G}$ = 54
J(ε)
G(ε)
EMITTANCE
ε

Fig. 10 a

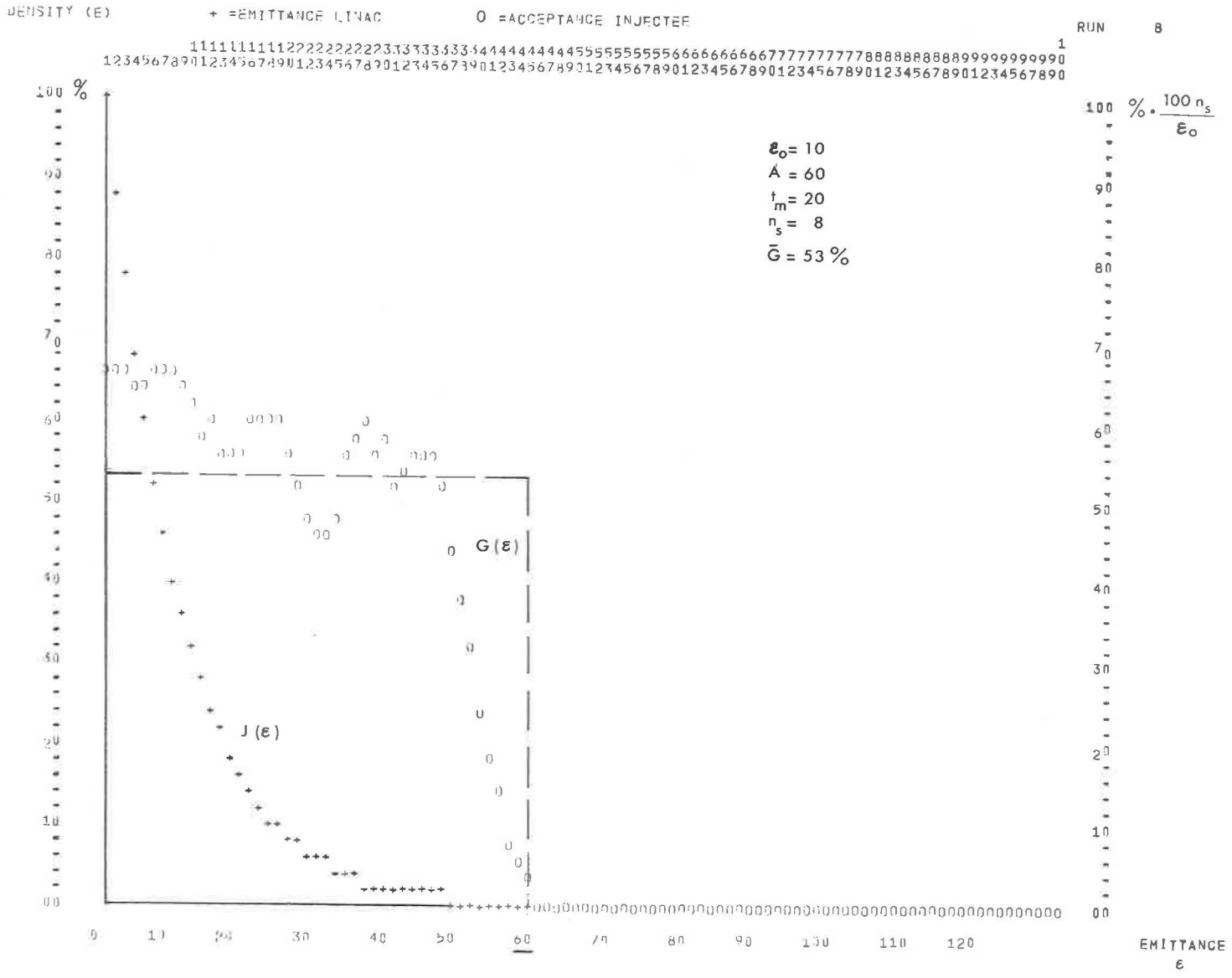
DENSITY (E)
+ =EMITTANCE LINAC
O =ACCEPTANCE INJECTEE
RUN 8
%
ε_o= 10
A = 60
t_m= 20
n_s = 8
$\bar{G}$ = 53 %
G(ε)
J(ε)
$\% \cdot \frac{100\, n_s}{\varepsilon_o}$
EMITTANCE
ε

Fig. 10b

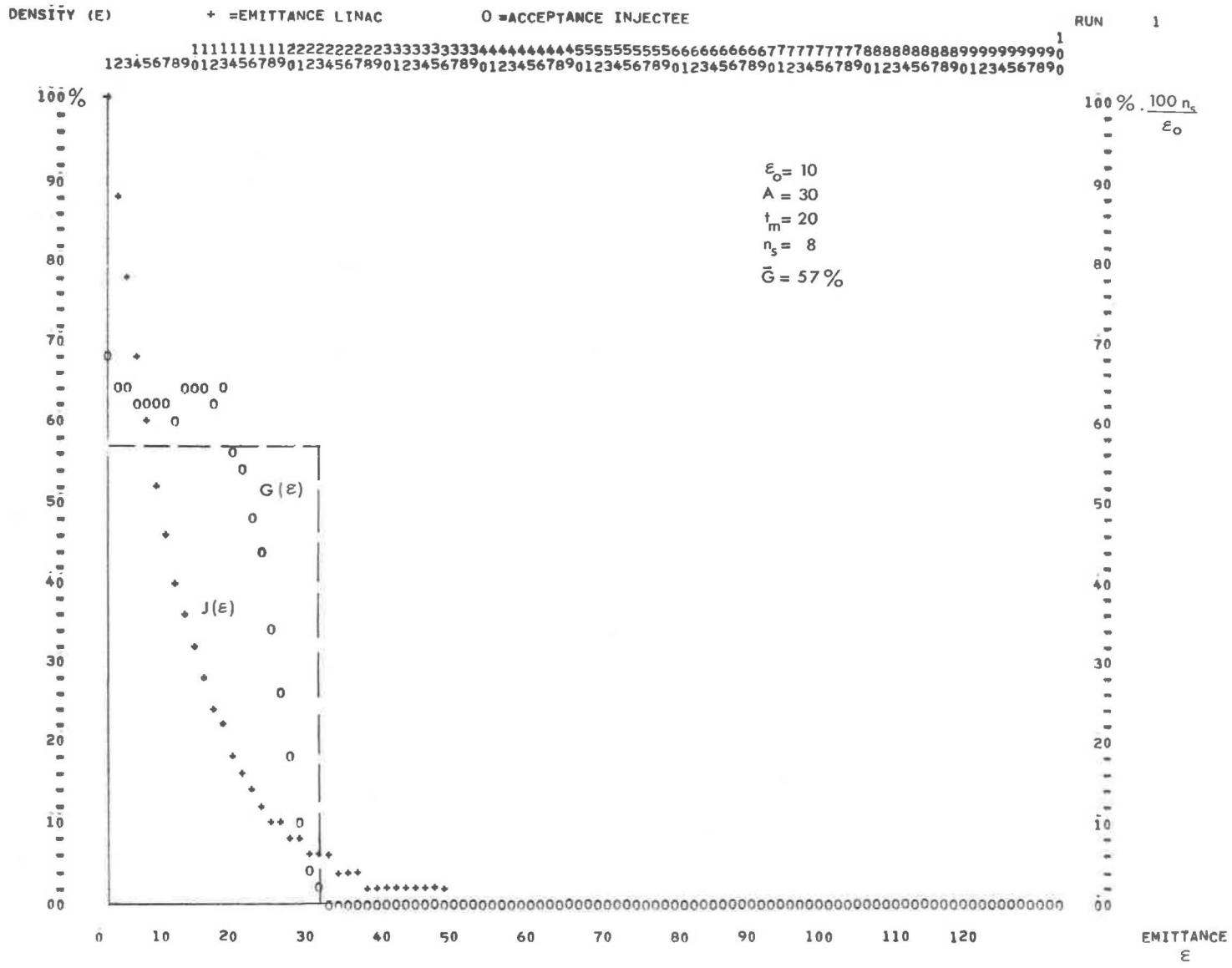
DENSITY (E)
+ =EMITTANCE LINAC
O =ACCEPTANCE INJECTEE
RUN 1
100 %
100 % . 100 n_s / ε_o
ε_o = 10
A = 30
t_m = 20
n_s = 8
G = 57 %
G(ε)
J(ε)
EMITTANCE
ε

Fig. 10 c

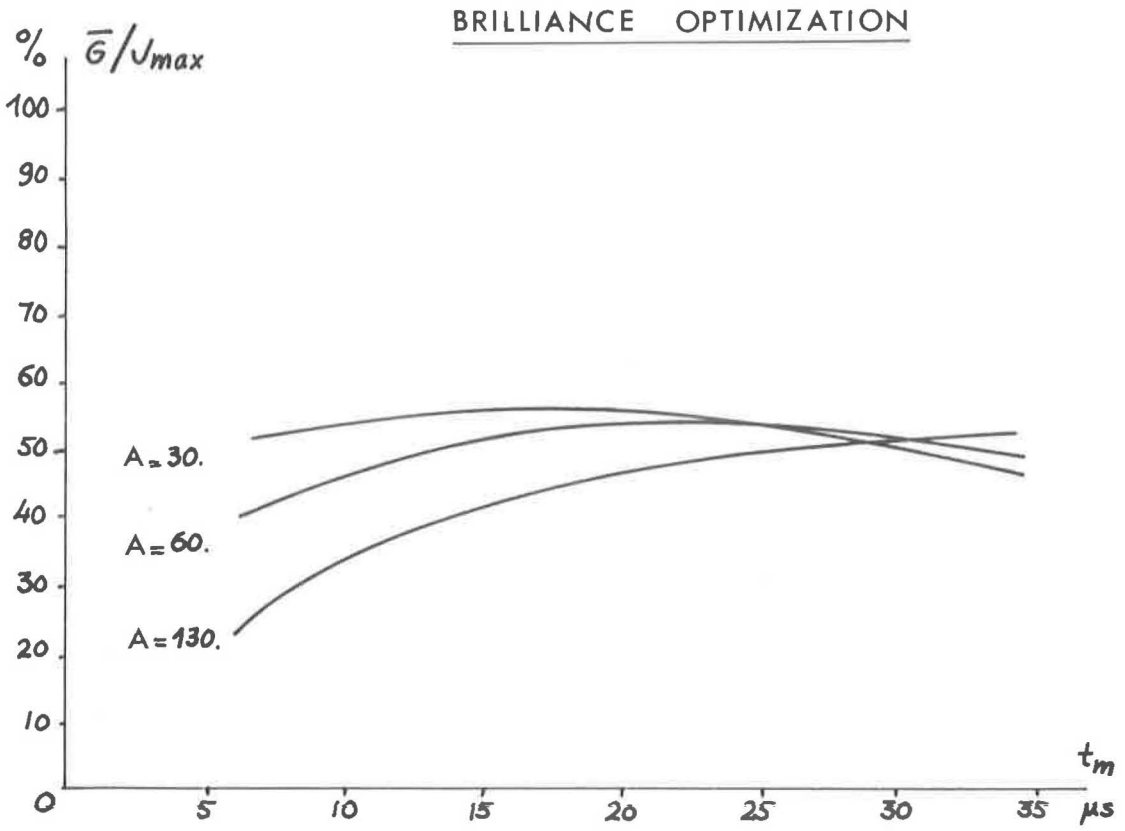
BRILLIANCE OPTIMIZATION
% $\overline{G}/J_{max}$
100
90
80
70
60
50
40
30
20
10
0
A = 30.
A = 60.
A = 130.
5
10
15
20
25
30
35
t_m
µs

Fig. 11

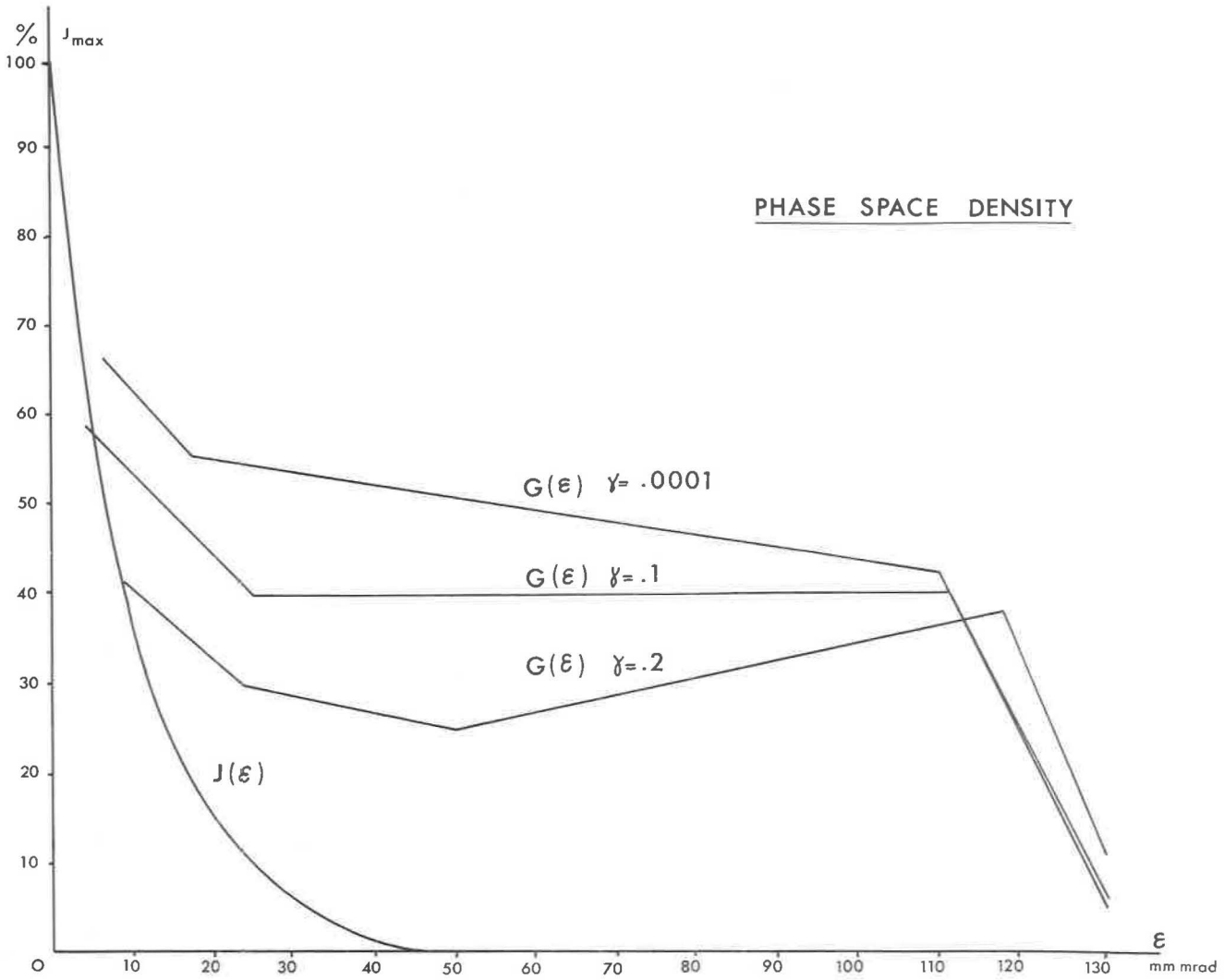
PHASE SPACE DENSITY
% J_{max}
100
90
80
70
60
50
40
30
20
10
0
10
20
30
40
50
60
70
80
90
100
110
120
130
ε
mm mrad
G(ε) γ= .0001
G(ε) γ= .1
G(ε) γ=.2
J(ε)

Fig. 12

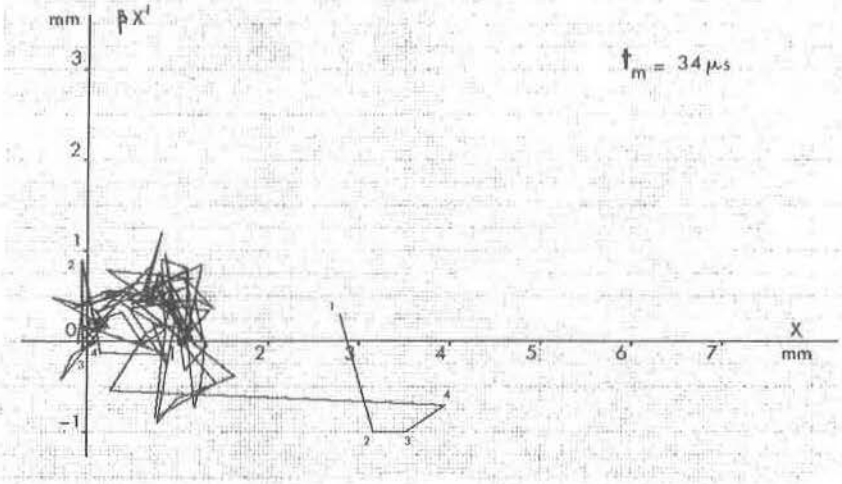

Fig.13a

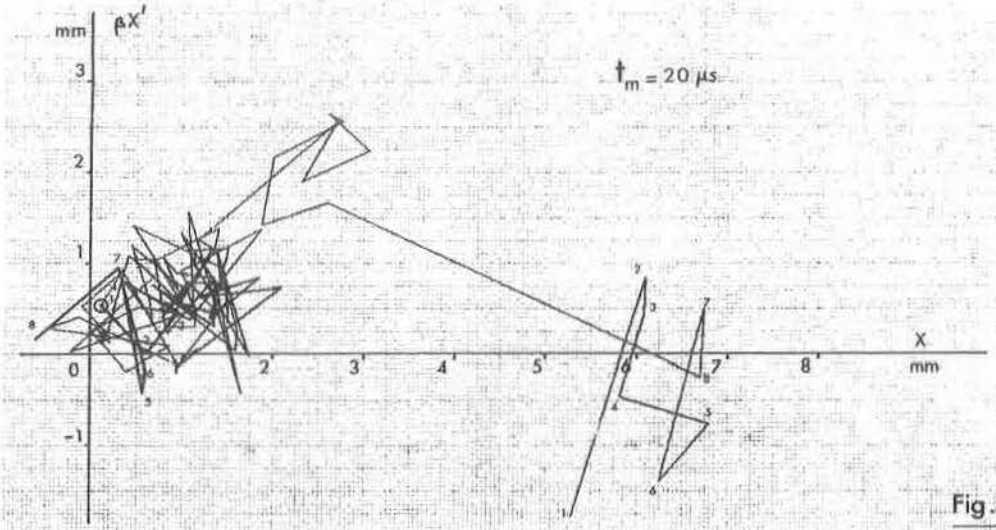

Fig.13b

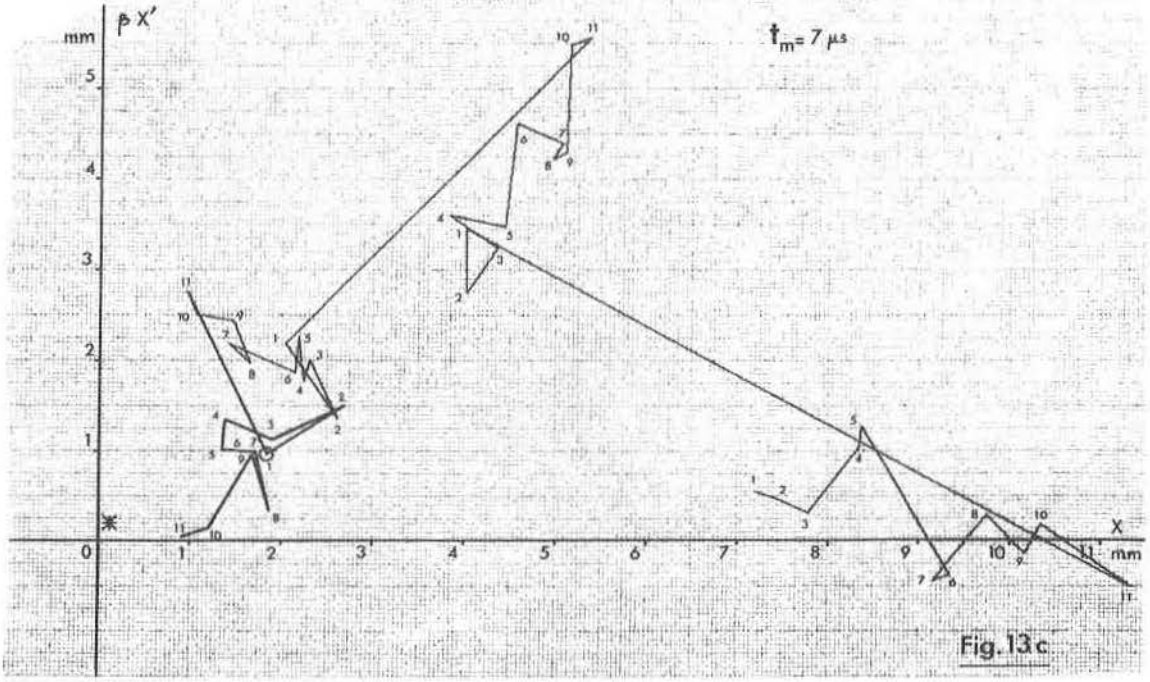

Fig.13c